

Letters

Bubble Colloidal AFM Probes Formed from Ultrasonically Generated Bubbles

Ivan U. Vakarelski,[†] Judy Lee,[†] Raymond R. Dagastine,^{*,‡} Derek Y. C. Chan,^{§,||,⊥}
Geoffrey W. Stevens,[‡] and Franz Grieser^{*,†}

Particulate Fluids Processing Centre, School of Chemistry, Department of Chemical and Biomolecular Engineering, and Department of Mathematics and Statistics, University of Melbourne, Parkville, Victoria 3010, Australia, Department of Mathematics, National University of Singapore, Singapore 117543, and Institute of High Performance Computing, 1 Science Park Road, Singapore 117528

Received October 15, 2007. In Final Form: November 30, 2007

Here we introduce a simple and effective experimental approach to measuring the interaction forces between two small bubbles ($\sim 80\text{--}140\ \mu\text{m}$) in aqueous solution during controlled collisions on the scale of micrometers to nanometers. The colloidal probe technique using atomic force microscopy (AFM) was extended to measure interaction forces between a cantilever-attached bubble and surface-attached bubbles of various sizes. By using an ultrasonic source, we generated numerous small bubbles on a mildly hydrophobic surface of a glass slide. A single bubble picked up with a strongly hydrophobized V-shaped cantilever was used as the colloidal probe. Sample force measurements were used to evaluate the pure water bubble cleanliness and the general consistency of the measurements.

Interaction forces between small gas bubbles are important in a number of scientific, medical, and technological developments, yet many aspects of these interactions remain poorly understood.^{1–3} Direct measurements of such forces have been reported using the atomic force microscopy (AFM) colloidal probe technique;⁴ however, these have been restricted to cantilever-attached solid particles and a large bubble (of a few hundred

micrometers) fixed on the substrate surface.^{5–8} Here we introduce a simple and effective experimental approach to extend the colloidal probe technique to cantilever-attached bubbles and surface-attached bubbles of various sizes. By using an ultrasonic source, we generated numerous bubbles on a mildly hydrophobic surface of a glass slide sample (Figure 1a). A single bubble was then picked from the surface with a strongly hydrophobized V-shaped cantilever (Figure 2b), and the interaction between the cantilever bubble and a surface bubble or another surface sample was measured.

The critical factor for the success of this procedure was the precise degree of hydrophobicity of the glass surface. It was not possible to generate bubbles on very hydrophilic surfaces (water contact angle of less than 10°), and for more hydrophobic surfaces (water contact angle of more than 30°), it was not possible to

* Corresponding authors. (R.R.D.) E-mail: rrd@unimelb.edu.au. Phone: +61-3-8344-4704. Fax: +61-3-8344-4153. (F.G.) E-mail: franz@unimelb.edu.au. Phone: +61-3-8344 6708. Fax: +61-3-9347 5180.

[†] School of Chemistry, University of Melbourne.

[‡] Department of Chemical and Biomolecular Engineering, University of Melbourne.

[§] Department of Mathematics and Statistics, University of Melbourne.

^{||} National University of Singapore.

[⊥] Institute of High Performance Computing.

(1) Ivanov, I. B.; Dimitrov, D. S. *Thin Liquid Films: Fundamentals and Applications*; Ivanov, I. B., Ed.; Marcel Dekker: New York, 1988.

(2) Lohse, D. *Phys. Today* **2003**, *56*, 36.

(3) Crag, V. S. J. *Curr. Opin. Colloid Interface Sci.* **2004**, *9*, 178.

(4) Ducker, W. A.; Senden, T. J.; Pashley, R. M. *Nature* **1991**, *353*, 239.

(5) Butt, H.-J. *J. Colloid Interface Sci.* **1994**, *166*, 109.

(6) Ducker, W. A.; Xu, Z.; Israelachvili, J. N. *Langmuir* **1994**, *10*, 3279.

(7) Gillies, G.; Michael Kappl, M.; Butt, H.-J. *Adv. Colloid Interface Sci.* **2005**, *114–115*, 165.

(8) Johnson, D. J.; Miles, N. J.; Hilal, N. *Adv. Colloid Interface Sci.* **2006**, *127*, 67.

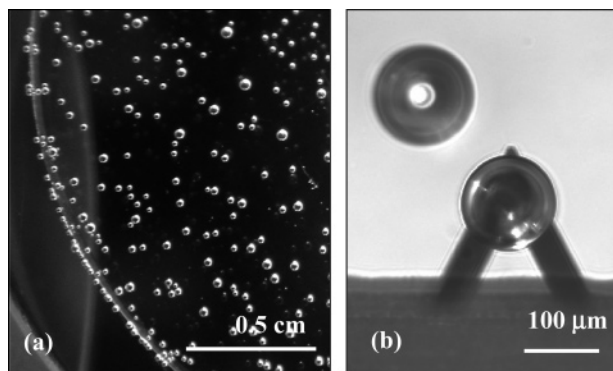


Figure 1. (a) Picture of a glass slide substrate covered with ultrasound-generated bubbles. (b) Optical microscopy image of a V-shaped cantilever with an attached air bubble and a second bubble anchored to the glass surface below.

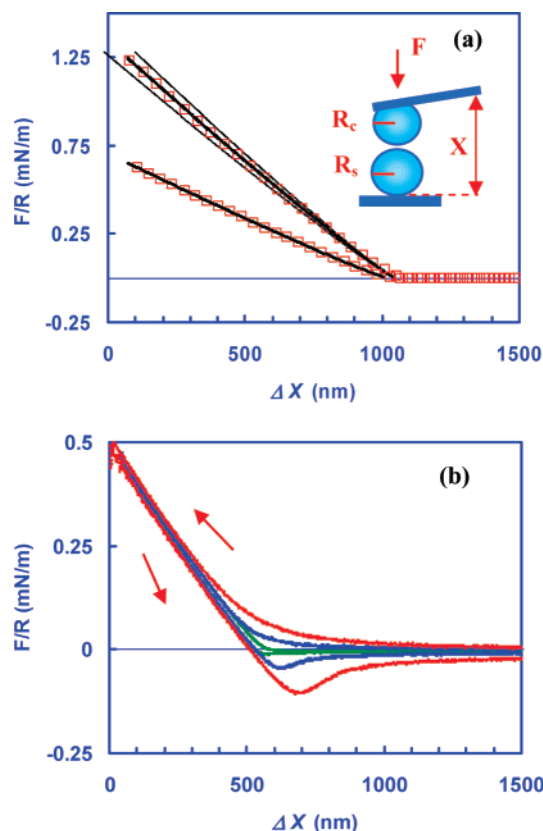


Figure 2. (a) Forces between two bubbles approaching at $1 \mu\text{m/s}$ piezo scan velocity in aqueous solutions of 1 mM NaNO_3 (upper data – cantilever-unperturbed bubble radius $R_c = 57 \mu\text{m}$, surface-unperturbed bubble radius $R_s = 65 \mu\text{m}$), and 10 mM SDS (lower data – $R_c = 57 \mu\text{m}$ and $R_s = 74 \mu\text{m}$). Solid lines are theoretical fits with $\gamma = 38.5 \text{ mN/m}$ in the SDS case and $\gamma = 71 \text{ mN/m}$ for the pure water case with the thin lines corresponding to $\gamma = 71 \pm 5 \text{ mN/m}$. (b) Approach (upper branches) and retraction (lower branches) forces between two bubbles ($R_c = 63 \mu\text{m}$ and $R_s = 95 \mu\text{m}$) in an aqueous solution of 1 mM NaNO_3 and piezo scan velocities of $1 \mu\text{m/s}$ (green), $10 \mu\text{m/s}$ (blue), and $30 \mu\text{m/s}$ (red). Forces were scaled by $R = R_c R_s / (R_c + R_s)$.

transfer the bubble to the cantilever. Only those bubbles attached to surfaces that were significantly more hydrophilic than a cantilever could be transferred successfully onto a cantilever. The contact area with the bubble is restricted by the cantilever dimensions despite the much higher hydrophobicity of the cantilevers (contact angle of more than 100°). Glass slides were mildly hydrophobized by dipping them for 5–20 s in a 3 mM solution of octadecyltrichlorosilane (OTS) in heptane to give the

surface hydrophobicity characterized by water contact angles in the $10\text{--}30^\circ$ range. (See Supporting Information for details.) After thorough cleaning, the slides were transferred in a Petri dish and covered with water. The Petri dish was positioned in an ultrasonic device (ELAC Nautik, GmbH) with the dish bottom a few millimeters above the ultrasonic transducer. A 647 kHz frequency signal of 6 W output power was applied until air bubble formation over the glass sample surface was observed in about 10 to 30 s. It was important to stop the sonication once the bubbles appeared because over-exposure resulted in the removal of the bubbles from the surface and no new bubbles would be formed. This behavior was most probably due to the degassing of the water. An example of a glass substrate covered with ultrasound-generated bubbles is shown in Figure 1a. The bubble size ranged from several tens to several hundred micrometers, and bubbles in the $90\text{--}120 \mu\text{m}$ range were optimum for transferring to the AFM cantilever.

Bubble cantilever attachment and force measurement experiments were carried out on an MFP-3D Asylum AFM. This AFM configuration allows the Petri dish to be placed on the sample stage. The integrated bottom view optical system of this AFM and the independent X–Y movement of the sample stage facilitated the bubble attachment manipulation. V-shaped tipless cantilevers (DI, NP-O) were hydrophobized by dipping them into 3 mM solutions of OTS in heptane for about 20 min. For the bubble experiments, we preferred the $196 \mu\text{m}$ long cantilevers with a nominal spring constant of 0.12 N/m . Bubble attachment was achieved by lowering the cantilever over a surface-attached bubble, pressing the bubble with the front part of the cantilever, and pulling back. Because of the higher hydrophobicity of the cantilever, the bubble was pulled from the surface and stayed attached on the lower side of the cantilever. An example of the cantilever-attached bubble is shown in Figure 1b.

In principle, the gas bubbles are thermodynamically unstable and will dissolve in water, with the smaller bubbles dissolving faster.⁹ Nevertheless, we found that for bubbles in the size range of $90\text{--}120 \mu\text{m}$ the dissolution was slow enough to allow repeat measurements, typically from a few to about 15–20 min under pure water conditions and longer after surfactant addition. Thereafter, the bubbles shrink rapidly. Indeed, these dissolution rates will depend on the gas saturation level of the aqueous phase.⁹ Another critical issue was the cleanliness of the bubble surface because gas bubbles in pure water are known to be easily contaminated. Our method has the advantage of generating the bubbles in the bulk of the solution, thus avoiding contact with possible contamination sources and at the same time creating multiple bubbles that in effect decrease the level of contamination compared to that of single-bubble techniques.^{5–8} Indeed, the present force measurement method can be used to identify the cleanest bubbles in pure water.

In Figure 2a,b, we present sample results of force measurements between two bubbles at different scan rates and solution conditions. The data collection and transformation were the same as for the standard AFM force measurement experiments and particularly for the case of a deformable surface (e.g., two emulsion droplets^{10–12}). Data are present as forces scaled by the mean unperturbed bubble radius vs relevant piezo displacement (inset in Figure 2a). In Figure 2a, we compare the interaction

(9) Epstein, P. S.; Plesset, M. S. *J. Chem. Phys.* **1950**, *18*, 1505.

(10) Dagastine, R. R.; Stevens, G.; Chan, D. Y. C.; Grieser, F. *J. Colloid Interface Sci.* **2004**, *273*, 339.

(11) Dagastine, R. R.; Manica, R.; Carnie, S. L.; Chan, D. Y. C.; Stevens, G. W.; Grieser, F. *Science* **2006**, *313*, 210.

(12) Clasohm, L. Y.; Vakarelski, I. U.; Dagastine, R. R.; Chan, D. Y. C.; Stevens, G.; Grieser, F. *Langmuir* **2007**, *23*, 9335.

force during approach between two bubbles in pure water (1 mM NaNO₃ background electrolyte) and in 10 mM solutions of sodium dodecylsulfate (SDS). In both cases, the bubble surfaces were charged,¹³ and a stable aqueous film separated the approaching bubbles. The lower slope in the case of forces in the presence of SDS reflects the lower interfacial tension of the bubbles and the resulting increase in deformability. The solid lines are fits with a theoretical model originally developed for the case of emulsion droplet interactions in an AFM-configured experiment.¹⁴ The model is based on the Stokes–Reynolds theory of thin film drainage and the Young–Laplace equation of drop deformation. Two simple analytical limits of this model have been derived. Here, we use the force-displacement relationship derived for the limiting case of a large repulsive force (in the context of surface force measurements) but low capillary numbers or drive velocities, where a stable dynamic film forms between the interacting interfaces (Supporting Information for model and fitting procedure details). In the reference case of SDS solution, the surface tension $\gamma = 38.5$ mN/m was well defined, and from the fit we determine the cantilever spring/detector sensitivity factor that for the case of large bubbles could significantly differ from that for an end-loaded cantilever.¹⁵ That value was then input into the pure water data fit to estimate the surface tension with the best fit obtained for $\gamma = 71$ mN/m. The closeness of the value to that of pure water, $\gamma = 72.5$ mN/m, confirms the cleanliness of the bubble surface. In Figure 2b, we illustrate the dynamic effects on the

interaction between two bubbles in a surfactant-free aqueous solution of 1 mM NaNO₃. The hydrodynamic effects are similar to the one observed with two emulsion droplets,¹⁰ showing a force increase with an increase in the velocity between the approaching bubbles and a characteristic minimum upon retraction. However, the correct theoretical interpretation of these data might require further extension of the model used for emulsion droplets¹¹ to account for the bubble compressibility and boundary conditions of surfactant-free liquid surfaces.

The bubble colloidal probe technique introduced here opens new investigation opportunities by allowing the direct measurement of the total force acting on a single microscopic bubble in both static and hydrodynamic regimes. The AFM probe has also allowed us to examine the interaction between bubbles at speeds overlapping those of Brownian motion. This provides details on how bubbles interact under natural conditions. Furthermore, these measurements can complement established methods such as interferometric thin liquid film cell techniques¹⁶ and more recent bubble–surface methods.^{17,18}

Acknowledgment. This work has been supported in part by the Particulate Fluids Processing Centre, a Special Research Centre of the Australian Research Council.

Supporting Information Available: Complete experimental details and appendix consisting of fitting equations and parameters used. This material is available free of charge via the Internet at <http://pubs.acs.org>.

LA7032059

(13) Choa, S.-H.; Kimb, J.-Y.; Chuna, J.-H.; Kima, J.-D. *Colloids Surf., A* **2005**, *269*, 28.

(14) Manica, R.; Connor, J. N.; Dagastine, R. R.; Carnie, S. L.; Horn, R. G.; Chan, D. Y. C. *Phys. Fluids*, submitted for publication, 2007.

(15) Vakarelski, I. U.; Edwards, S. A.; Dagastine, R. R.; Chan, D. Y. C.; Stevens, G. W.; Grieser, F. *Rev. Sci. Instrum.* **2007**, *78*, 116102.

(16) Derjaguin, B. V. *Theory of Stability of Colloids and Thin Films*; Consultants Bureau: New York, 1989.

(17) Pushkarova, R. A.; Connor, J. N.; Horn, R. G. *Colloids Surf., A* **2005**, *261*, 147.

(18) Connor, J. N.; Horn, R. G. *Proceedings of the Australian Institute of Physics 17th National Congress*: Brisbane, Australia, 2006; Paper No. 0275.